ELSEVIER

Carbohydrate Polymers 52 (2003) 53–65

Carbohydrate Polymers

www.elsevier.com/locate/carbpol

Fourier transform infrared microspectroscopic study of the chemical microstructure of corn and oat flour-based extrudates

Dirk Rainer Cremer[1], Gönül Kaletunç*

Department of Food, Agricultural, and Biological Engineering, The Ohio State University, 590 Woody Hayes Dr., Columbus, OH 43210, USA

Received 7 March 2002; revised 9 September 2002; accepted 9 September 2002

Abstract

The spatial distribution of starch, protein, and lipid domains (chemical microstructure) in corn and oat flour-based extrudates was investigated in 8 μm thick cross-sections of the products by FTIR-microspectroscopy mapping experiments. The results reveal an even starch distribution in all extrudates investigated confirming that starch forms a continuous phase in cereal-based extrudates. Proteins were the least evenly distributed among the three components. Also, small, protein rich domains of 70 μm diameter were detected in the microstructure of the extrudates. Starch and protein distributions were always inversely related to each other. The lipids in oat flour-based extrudates were less evenly distributed than the starch, but more evenly than the proteins. Lipid distribution was neither correlated with starch nor with protein distribution.

Keywords: Cereals; Extrusion; Microstructure; FTIR; Microspectroscopy

1. Introduction

Expanded snack foods and ready-to-eat breakfast cereals are manufactured using high-temperature, short time, extrusion cooking process. These products are porous, brittle, solid foams fixed in a glassy state at about 6–10% moisture content and ambient temperature. Porous structure is comprised of air pockets or air cells surrounded by solid material referred to as cell walls. The product properties are influenced by extruder operational parameters such as barrel temperature, screw configuration, screw speed, and die shape as well as raw material formulation, namely the water, protein, starch and lipid content (Bhatnagar & Hanna, 1994a,b; Chinnaswamy & Hanna, 1988, 1990; Faubion & Hoseney, 1982a,b; Ghorpade, Bhatnagar, & Hanna, 1997). Furthermore, additives, including sugars and proteins influence the extrudate properties (Barret, Kaletunç, Rosenburg, & Breslauer, 1995; Faubion & Hoseney, 1982b; Maurice & Stanley, 1978; Skierkowski, Gujska, & Khan, 1990). Extrusion of cereal flours results in a destruction of the starch granule, degradation of the starch polymer chains, denaturation and aggregation of proteins, formation of starch–lipid and protein–lipid complexes and protein–protein cross-linking (Bhatnagar & Hanna, 1994a,b; Chai, Disady, & Rubin, 1995; Colonna & Mercier, 1983; Ho & Izzo, 1992; Kazemzadeh, Aguilera, & Rhee, 1982; Mercier, Charbonniere, Gallant, & Guilbot, 1979; Mercier & Feillet, 1975; Meuser, Pfaller, & Van Lengerich, 1987; Noguchi, 1989; Schweizer, Reimann, Solms, & Eliasson, 1986; Singh & Smith, 1997). In extrudates the starch forms a continuous amorphous phase while the proteins are present as a discontinuous phase (Hermansson, 1988). Using light microscopy with differential staining of wheat flour extrudates, Kaletunç (1999) showed that the proteins form fibrous filaments aligned in the extrusion direction. Batterman-Azcona and Hamaker (1998) report that during extrusion of corn meal α-zeins are partly released from the protein bodies, merge together and form a filamentoid network. Other studies on pea and soy flour (Ben-Hdech, Gallant, Bouchet, Guegeun, & Melcion, 1991; Noguchi, 1989) also reveal that during extrusion protein bodies aggregate and fuse to form a fibrous protein matrix giving rise to a 'structural segregation' within the product.

Wetzel (1993), Wetzel and Fulcher (1990), and Wetzel and Reffner (1993) utilized FTIR-microspectroscopy for

* Corresponding author. Fax: +1-614-292-9448.
E-mail address: kaletunc.1@osu.edu (G. Kaletunç).
[1] Present address: Degussa BioActives, Lise-Meitnerstr. 34, 85354 Freising, Germany.

0144-8617/03/$ - see front matter © 2002 Elsevier Science Ltd. All rights reserved.
PII: S0144-8617(02)00266-7

the evaluation of the chemical microstructure of foods. These researchers demonstrated that FTIR-microspectroscopy makes it possible to obtain in situ spectra of thin-sections of food materials with a spatial resolution as small as 10 μm. Wetzel and Reffner (1993) using a moving stage conducted mapping experiments on thin-sections of corn and wheat to demonstrate the existence of chemical differences among pericarp/aleurone/endosperm. They also showed from the spatially resolved FTIR spectra that the lipid content is higher in the pericarp than in the endosperm and that the carbohydrate density is highest in the central endosperm. Durrani and Donald (1994, 1995) and Durrani, Prystupa, and Donald (1993), used FTIR-microspectroscopy to study the chemical composition of phase-separated amylopectin/gelatin gels. Durrani and Donald (1995) applied the method of partial least-squares analysis to FTIR data to generate quantitative data in order to construct ternary phase diagram for phase separated amylopectin–gelatin gels in terms of weight percentages of gelatin, amylopectin, and water. Noguchi (1989) and Stanley (1989) reported changes in the protein bands of IR spectra of protein containing food material as a result of extrusion process. Kaletunç (1999) utilized FTIR-microspectroscopy to study the distribution of starch and protein in the microstructure of wheat flour extrudates. Mousia, Farhat, Pearson, Chesters, and Mitchell (2001) studied extruded gelatin–amylopectin blends using FTIR-microspectroscopy to monitor the spatial relative distributions of the two components in the extruded product.

Oat products are getting more popular due to their claimed cholesterol-lowering properties. However, unlike most cereal flours, an expanded structure cannot be obtained with only oat flour due to its high level of lipid and soluble gums. Therefore, typically oat flour is used by blending with other cereal flours for extruded products (Liu, Hsieh, Heymann, & Huff, 2000; Singh & Smith, 1997). In this study, corn is used in combination with oat since corn is known to produce well-expanded structure during extrusion.

The objective of this study is to investigate the distribution of starch, protein and lipid domains in the microstructure of extrudates prepared from corn and oat (100% corn, 100% oat, 1:1 mixture of corn and oat). To this end, FTIR-microspectroscopy is employed to spatially resolve chemical information about the microstructure of these products.

2. Materials and methods

2.1. Cereal flours

Degerminated corn flour with a starch, protein ($N \times 6.25$) and lipid content of 78.6, 6.0 and 2.2%, respectively, was obtained from the Lauhoff Grain Company, Danville, Illinois. Oat flour, containing 68.6, 13.5 ($N \times 6.25$) and 7% of starch, protein and lipid was obtained from The Quaker Oats Company, Chicago, Illinois.

2.2. Extrusion

Corn flour, oat flour and a 1:1-blend of corn and oat flours were processed in a Clextral BC 45 (Clextral Co., Firminy, France) twin-screw extruder (screw diameter 56 mm, screw length 1 m). The flours were metered in with a volumetric feeder. The feed rate was kept constant at 27.2 kg/h. The moisture level during extrusion was held constant at 20%. The water was introduced to the extruder by a feed pump immediately after the flour feed zone. The screw speed was set at 250 rpm. The temperature profile of the four thermally regulated modules in the extruder barrel was ambient, 93, 110 and 149 °C. A die of 5 mm diameter was used. Following extrusion, the extrudates were cooled down to ambient temperature and were then stored in polyethylene bags at ambient temperature.

The specific mechanical energy (SME) was calculated using the equation provided in the extruder manual

$$\mathrm{SME(Wh/kg)} = \frac{(0.9)(U)[A(\mathrm{amps})][N(\mathrm{rpm})]}{[N_{\max}(\mathrm{rpm})][Q(\mathrm{kg/h})]}$$

where, U is the maximum voltage, A is the amperage, N and $N_{\max}$ are the screw speed and maximum screw speed, Q is the feed rate. The SME values were calculated to be 911 kJ/kg for corn flour, 547 kJ/kg for corn/oat blend, and 457 kJ/kg for oat flour.

2.3. FTIR-microspectroscopy

2.3.1. Specimen preparation

A Microm HM 505E (Microm International GmbH, Walldorf, Germany) microtome was used to prepare thin-sections of the extrudates. Due to the brittle nature of the extrudates, slices of approximately 1 cm length were embedded in Tissue Tek (Sakura FineTek Inc., Torrance, CA, USA) prior to the cryo-thin-sectioning. Extrudate cross-section of 8 μm thickness was obtained and placed between two BaF_2-windows (SpectraTech Inc., Shelton, CT, USA) of 2.5 cm diameter and 3 mm thickness. A rubber o-ring was used as a spacer between the windows. Since Tissue Tek shows some prominent absorption bands in spectral regions that were of interest for this study, only those areas of the specimen were analyzed that proved to be free of embedding medium. Parts of the specimen that were soaked with Tissue Tek could easily be identified by their altered light refraction when viewing the specimen in the visible light mode under the microscope.

Prior to the FTIR-microspectroscopic investigation, the specimens were stored 5 days over a saturated magnesium chloride (Fisher Scientific, Columbus, OH, USA) solution (relative humidity: 32% at 20 °C) in a dessicator in order to assure constant moisture content. The final moisture contents (wet basis) of the specimens of extruded products used for FTIR measurements were 9.0 (corn, corn/oat blend) and 9.5% (oat). These values

were calculated by determining the initial moisture content of the extrudates by means of freeze-drying and by determining the final weight of extrudate samples at a relative humidity of 32%.

2.3.2. Mapping experiments

An FTIR spectrometer (Equinox 55, Bruker Instruments Inc., Billerica, MA) with an attached microscope was used to record spectra of extrudates. The instrument was equipped with a mercury cadmium telluride (MCT-) detector which was cryostated with liquid nitrogen. The setup of the microscope allowed either to view the specimen in the visible mode or to switch to the IR mode for measurements. A $\times 15$ non-infrared absorbing objective lens was used during FTIR data acquisition. The specimen environment was purged with dry nitrogen gas to drive out CO_2 and moisture. In the visible mode an additional $\times 4$ objective and an $\times 10$ condenser lens was used resulting in a 40 or 150 $\times$ magnification. With a video camera (CCD-IRIS, Sony, Japan) mounted into one of the condenser lens positions it was possible to take photomicrographs of specimen spots prior to the FTIR data collection. The software used for the video photomicrograph processing was SMTV II, version 1.1 (FAST Electronic GmbH, Munich, Germany). Additionally a regular stereo microscope (SMZ-U, Nikon Inc., Melville, NY, USA) with a 10–75 $\times$ magnification and equipped with a camera (type N6000, Nikon Inc., Melville, NY, USA) was used in order to locate the position of a mapped specimen area within the entire extrudate cross-section which could not be accomplished with the FTIR-microscope.

The FTIR-microscope stage was movable in both directions of plane. It was controlled by a MCL-2 stage controller (Maerzhaeuser, Wetzlar, Germany) and the instrument software OPUS 3.0.2 (Bruker Analytik GmbH, Karlsruhe, Germany). This set-up allowed us to automatically acquire FTIR spectra at each preprogrammed x, y-location in a grid. This process is called mapping. The precision of the moving stage was 1 μm during mapping experiments. Spatial resolution of 66.7 μm for spectra collection was achieved using an aperture of 1.05. Mapping experiments of this study were performed using a rectangular grid and a point spacing of 20 μm resulting in a spectra overlap due to the larger aperture diameter. Individual spectra of specific loci and traces (definition given below) could be extracted from the acquired map for examination and comparison.

2.3.3. Mapping data acquisition

Infrared absorbance spectra were acquired in the transmission mode. In this mode the IR beam enters the specimen from the bottom, passes through it and finally reaches the detector. Spectra were collected between 4000 and 700 cm^{-1} at a 4 cm^{-1} resolution. The interferograms were co added and Fourier transformed using the Blackman-Harris 3-term apodization function. A spectrum of an empty portion of the BaF_2 window was used as background and was always scanned (256 scans) prior to the mapping data acquisition for specimen. Specimen spectra were averaged from 20 interferograms.

2.3.4. Mapping data analysis

The integration of the absorption bands of interest, which were the carboxylic ester carbonyl band at 1740 cm^{-1} (associated with lipids), the amide I and II bands at 1650 and 1550 cm^{-1}, (originating from proteins), and the carbohydrate bands between 1100 and 1000 cm^{-1}, (stemming from starch), was performed to a linear baseline defined between 1800 and 885 cm^{-1}. In order to account for thickness changes within the specimen, the integrated peak areas were normalized by the entire area of the fingerprint region (1800–885 cm^{-1}).

The integration results of absorption bands from each map were exported and further processed with Excel 97 (Microsoft Corporation, USA) and PSI Plot (version 4.54, Poly Software International, Salt Lake City, UT, USA). The exported data consisted of a spreadsheet of the spatial coordinates (reduced to one value for each x, y-pair) of the collected spectra (x-column) and the integration result of a functional group at the respective position (y-column). This data table, called trace, contained the spatial and the spectral information in the order given by the data acquisition matrix which was $x_1y_1,\ x_2y_1,\ x_3y_1,\ldots,x_my_1,\ x_1y_2,\ldots,x_my_2,\ldots,x_1y_n,\ldots,x_my_n$. Functional group surface plots were generated from the traces to visualize the information of the distribution of the individual components within a mapped specimen area (chemical microstructure).

2.3.5. Statistical analysis of mapping data

Statistical analysis of mapping data was conducted with the S-Plus, version 5.1 (MathSoft Inc., Cambridge, MA, USA) and the SAS, version 7 (SAS Institute Inc., Cary, NC, USA) software program. The mean values for carbohydrate (starch), protein and lipid band areas determined in individual maps were calculated and compared by ANOVA analysis and Kruskal Wallis test, which is the non-parametric analogue of ANOVA. The Kruskal Wallis test was performed when the mapping data were not normally distributed but skewed to the right or the left. However, mostly ANOVA and Kruskal Wallis tests yielded similar statistical results. An ANOVA model, assuming an unstructured covariance matrix, was used to account for correlations between the pairs of carbohydrate, protein, and lipid components.

The variability of the spatial distribution of a component was expressed in terms of the relative standard deviation (RSD). The RSD is defined as the standard deviation (SD) of a given set of measured data points divided by the respective mean value of that data set.

3. Results and discussion

3.1. Comparison of the average spectra of extrudates

Fig. 1 shows the spectra of corn, corn/oat and oat flour extrudates. Fifty spectra of each extrudate were averaged from 50 different locations within the cross-sections. All spectra showed a broad peak in the OH stretching region in the vicinity of 3400–3200 cm^{-1}. For some oat flour extrudates, the OH stretching region had a triangular shape as a result of a large contribution from NH stretching vibrations (symmetric 3180, asymmetric 3330 cm^{-1}) superimposing on the OH band. The higher lipid content of the oat/corn and oat flour extrudates resulted in a more pronounced CH stretching region. The main peak at 2927 cm^{-1} (CH_2 stretching, asymmetric) was accompanied by a smaller but very sharp second peak appearing at 2855 cm^{-1} (CH_2 stretching, symmetric). The smaller peak was not observed in the corn extrudate spectra. The higher lipid content of the oat and corn/oat flour extrudates was apparent from the ester carbonyl stretching band at 1744 cm^{-1} which almost disappeared in the corn flour extrudate spectra. However, a signal increase in the CH bending region (1469 cm^{-1}) with increasing lipid content was not detectable. A plot of the integrated carbonyl band as a function of the bulk lipid weight percentage in the extrudates gave a straight line ($r = 0.999$) implying that the Beer–Lambert law applies to the carbonyl band irrespective of the extrudate matrix in which it is measured.

The amide I bands (primarily C=O stretching vibrations) displayed their maxima at 1644 (oat, corn/oat) and 1650 cm^{-1} (corn), respectively. The amide II bands (largely NH bending vibrations) were observed at 1536 (corn, corn/oat) and 1531 cm^{-1} (oat). Comparison of the spectra of the extrudates from the present study with the spectra of corn endosperm reported by Wetzel (1993) showed that the amide II band of the extrudates was broader, less intense, more featureless and thus less well defined than the respective amide II band of the corn endosperm. A similar amide II band was observed for all of the extrudates investigated. The broadening of the amide II band may be related to protein random structures as can be derived from the spectra presented by Chittur (1998). Amide I band which typically occurs in the region 1600–1700 cm^{-1} has been shown to provide information about the secondary structure of proteins. Although the spectral features may vary slightly depending on the environment, structural distortion, and domain interactions, typically α-helical, β-sheet, and random structures are assigned to bands in the frequency ranges of 1650–1658, 1620–1635, and 1640–1650 cm^{-1} (Fabian & Schultz, 2000). The protein denaturation and even aggregation (Kazemzadeh et al., 1982) are expected to occur during extrusion. The aggregated polypeptides are reported to absorb at either 1615 or 1685 cm^{-1} (Fabian & Schultz, 2000) which both are considerably different than the amide I frequencies observed for the extrudates. Therefore, we can speculate that amide I maxima for the extrudates in this study

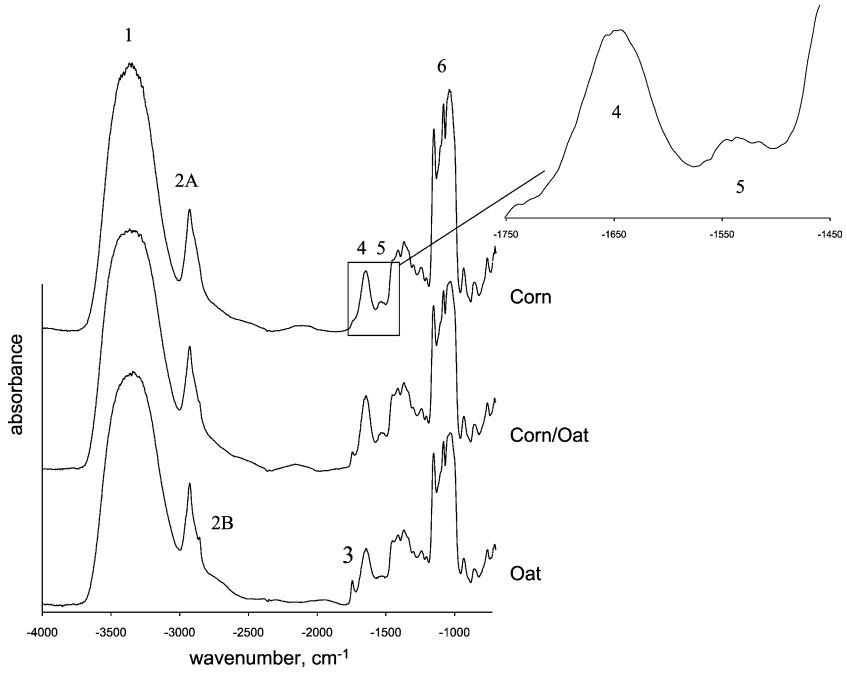

Fig. 1. Average spectra of corn, corn/oat and oat flour extrudates. Spectra were recorded at 50 different locations in the extrudate cross-sections with 20 scans/spectrum and a 67 μm circular aperture. 1 = OH, NH stretching region; 2A = CH stretching, asymmetric; 2B = CH stretching, symetric; 3 = ester carbonyl stretching; 4 = carbonyl stretching of secondary amides (amide I) and HOH deformation; 5 = NH in-plane bending of secondary amides (amide II); 6 = C–C–O, C–C, O–C–O stretching (sugar rings; carbohydrates (here: starch)).

indicate a random conformation but not an aggregated state for the proteins. Noguchi (1989) and Stanley (1989) also independently reported changes in the protein bands of extrudate spectra as a result of the extrusion processing and attributed them to changes in the peptide bonds due to extrusion.

The ratios of the integrated band intensities of amide I to amide II averaged from all maps increased from 3.6 (oat) and 3.7 (corn/oat), respectively, to 4.5 (corn) implying an increase in starch content from oat to corn. It is well established that the H–O–H bending vibrations of water absorb strongly near 1640 cm^{-1} around which the amide I band absorbs (Cooper & Knutson, 1995). Additionally a weak C–O–H deformation of the starch glucose ring contributes at 1650 cm^{-1}. Typically in proteins, the integral ratio of amide I:II can vary from 3:1 to 2:1. The ratio approaches 3:1 in the case of purely alpha-helical proteins and 2:1 in purely beta sheet proteins. Therefore it is reasonable to assume that starch and moisture can contribute to the amide I region and influence the ratio towards more amide I.

The carbohydrate fingerprint region in the vicinity of 1100–1000 cm^{-1} for all three products (corn, corn/oat and oat) exhibited three strong and characteristic peaks at (1151, 1154, 1154), (1082, 1081, 1080) and (1038, 1031, 1035) cm^{-1}. The ratio of the integrated band intensities for carbohydrate /amide II ranged from 22 (oat extrudate) and 23 (corn/oat extrudate) to 38 (corn extrudate). The higher ratio of starch to protein in corn extrudates is apparent from the comparison of oat and corn extrudate FTIR data. The marginal difference between the ratio of carbohydrate to amide II band areas for oat and corn/oat extrudates may be attributed to the different absorption coefficient of the proteins in these extrudates. Fabian and Schultz (2000) reported studies on polypeptides and proteins revealing the change in the molar absorptivities due to alteration of the polypeptide backbone structure.

3.2. Spatial distribution of starch, protein and lipid (compositional mapping)

3.2.1. Overview

Compositional IR mapping was performed on extrudate cross-sections. Preparation of the extrudate cross-section was observed to be the most crucial point. Complete cross-sections could be gained for the oat and corn/oat flour extrudate. The corn flour extrudate was too brittle to yield complete sections, however partial sections were obtained by increasing the amount of embedding medium prior to the thin sectioning. In the FTIR mapping experiments only embedding medium free areas were mapped because the embedding medium is known to absorb at frequencies of 1735, 1446, 1248 and 1098 cm^{-1}. The visible mode of the microscope was utilized to exactly locate a mapped area within the cross-section. Fig. 2 gives an example (oat flour extrudate) of the location of a mapped area in relation to the entire cross-section of extrudate.

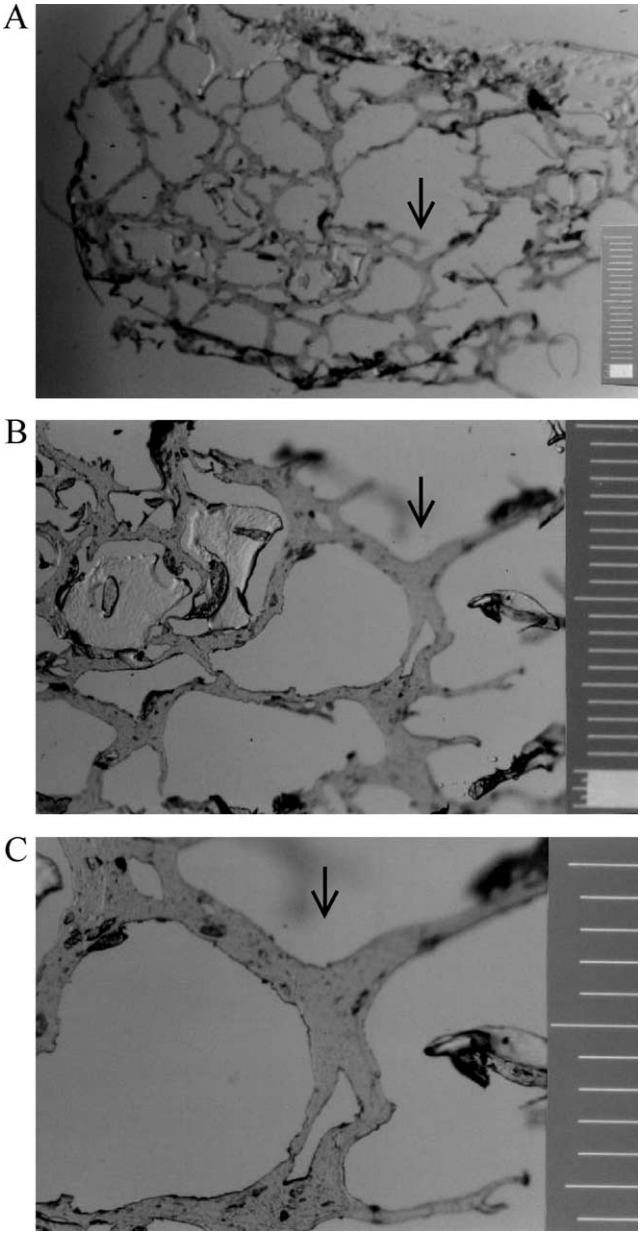

Fig. 2. Photomicrographs of an oat flour extrudate cross-section of 8 μm thickness. A = 15, B = 40 and C = 75 × magnification. A mapped area is indicated by an arrow. Scale: 100 μm between bars.

The maps were acquired from the extrudate cell walls and areas where these walls merged together. For the corn and corn/oat flour extrudates these areas were approximately located within a 3 mm radius (referred to as 'middle' section) from the outer diameter of the extrudate cross-sections. Maps from the oat flour extrudate were generated from the edge of the cross-section (peripheral section), from the middle, and from the central (center section) area of the cross-section. The section called

peripheral was defined as the outermost cell walls that were in direct contact with the die during the extrusion process. The extrudate diameters were 1.0 (oat), 1.7 (corn/oat) and 1.8 cm (corn), respectively. Fig. 3 shows photomicrographs of mapped cell wall areas of corn, corn/oat and oat flour extrudates. These photomicrographs were taken under the FTIR microscope with a 150× magnification. The structure was not stained. The dark spots in the cell wall structure seen in Fig. 3 are not related to compositional differences. They are rather related to subtle stray light effects that were caused by small size air inclusions. Mapped areas ranged from 110×150 to $250 \times 390\ \mu m^2$. Spectra recorded during mapping were averaged from 20 interferograms. This number of scans produced reliable and reproducible spectra and peak integration results. Comparing the RSD of the integrated peaks of interest (carbohydrate, amide I and II, and carbonyl band) obtained with 256 and 20 scans revealed that the average RSD increased from 0.7 to 2.0% with the reduction of scans. The integration method proved to reproduce the integration counts irrespective of the number of spectra scans (down to 10 scans). Similar observations were made by Hakuli, Kytoekivi, Lakooma, and Krause (1995). These authors investigated the influence of the number of scans on FTIR spectra integration results of volatile organic compounds analyzed by gas chromatography and found only a slight change in the average RSD when the scans were reduced from 100 to 10. We also determined signal/noise ratios (*S/N*) over the spectral range of 1950–1850 cm^{-1} from transmission spectra by fitting a parabola to the selected range. The *S/N* ratio was calculated as the root mean square SD from the nominal signal as defined by the fitted parabola. A comparison of a spectrum comprised of 256 scans with one of 20 scans showed that *S/N* decreased from 420 to 340.

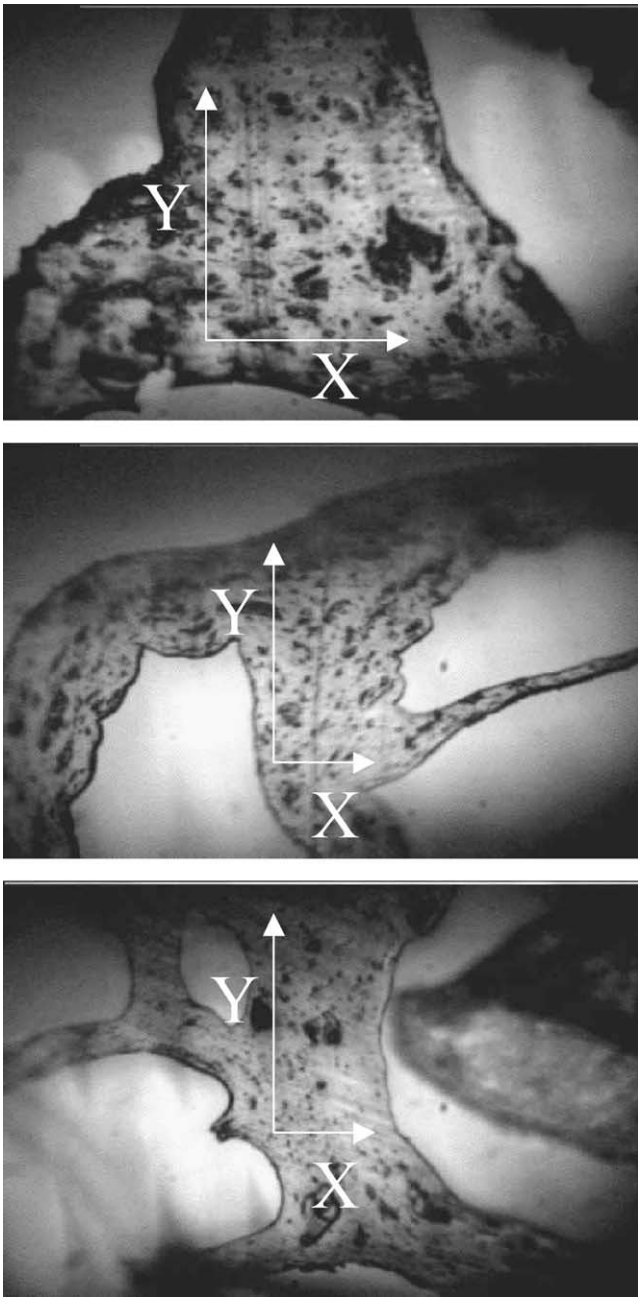

Fig. 3. Photomicrographs of *x*, *y*-mapped areas as indicated by rectangles in a corn (A), corn/oat (B)and oat flour (C) extrudate cross-section of 8 μm thickness. Magnification 150×.

The distribution of components present in the extrudates was reported as a function of *x*- and *y*-position. In Figs. 4, 5 and 7, the *z*-axis always represents the percent of the mean band area for the specific component. The mean band area was calculated using the entire set of mapping data acquired from the same type of extrudate.

3.2.2. Carbohydrate (starch) and protein distribution

The starch distributions in corn, corn/oat and oat extrudates were similar (Fig. 4). Corn flour extrudates have the largest cell wall thickness allowing the acquisition of maps of larger areas. It is apparent that the starch was evenly distributed throughout the mapped areas for all extrudates. The RSD values of the integrated starch bands were calculated to be 3.7 (corn), 6.3 (corn/oat) and 7.9% (oat). The increase in RSD from corn to oat may be due to the decrease in expansion of the product giving rise to a slightly more pronounced heterogeneity in the starch distribution. The data presented in Fig. 4 are in agreement with the light-microscopic findings of other investigators (Flint, 1994; Hermansson, 1988) and with the FTIR-microspectroscopic observations reported for wheat flour extrudates (Kaletunç, 1999). All of these investigators concluded starch to be the continuous phase while the proteins formed a discontinuous phase.

The protein distribution (amide II) was far less uniform, as can be seen in Fig. 4. The mean RSD of the protein (amide II) distribution was calculated to be 41 (corn), 36 (corn/oat) and 55% (oat) implying

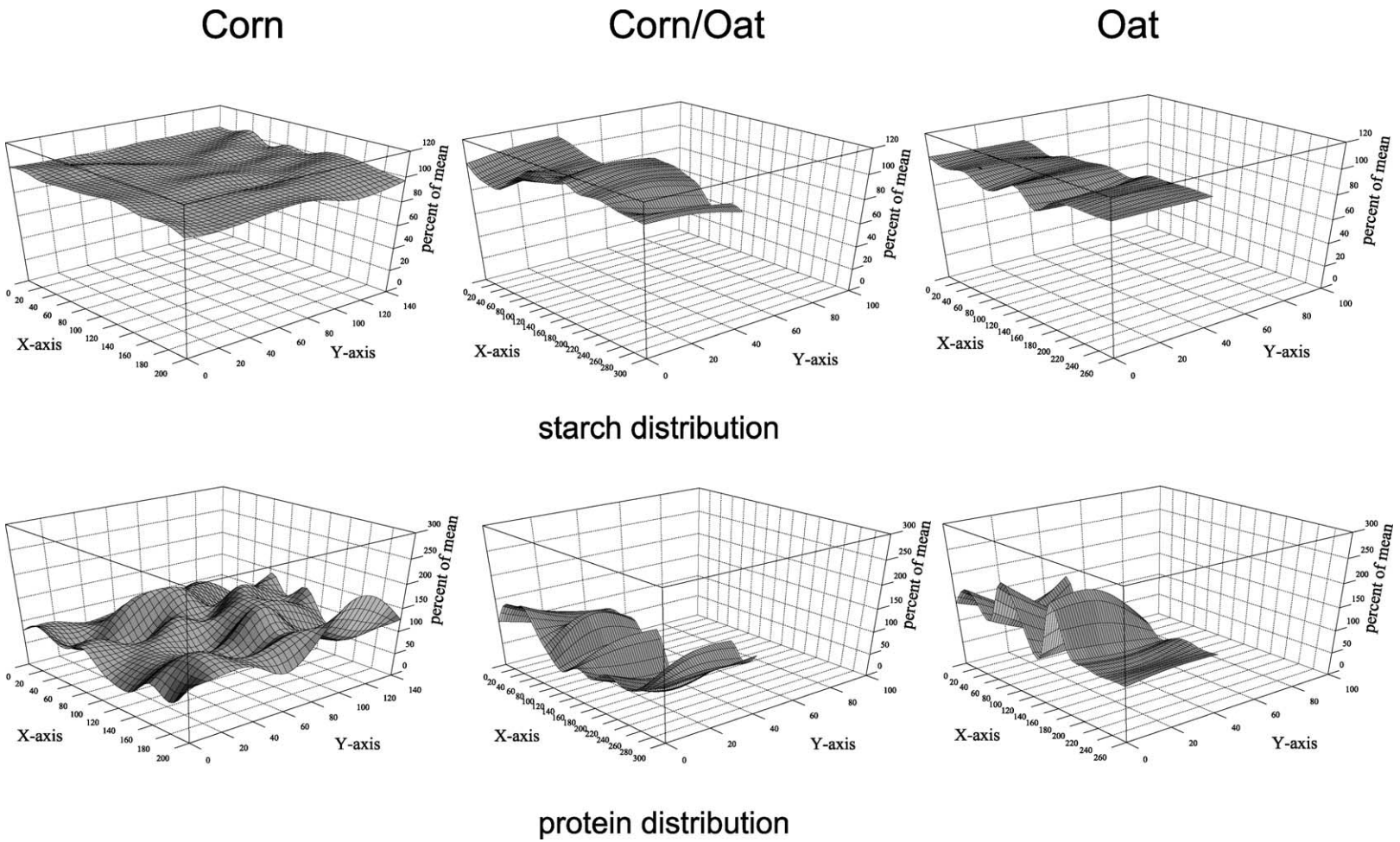

Fig. 4. 3D-surface plot of starch and protein (amide II) distributions in three different extrudate cross-sections of 8 μm thickness. Mapping data were acquired at regular intervals of 20 μm. Component concentrations were expressed as percent of the respective mean peak area as averaged from all maps acquired.

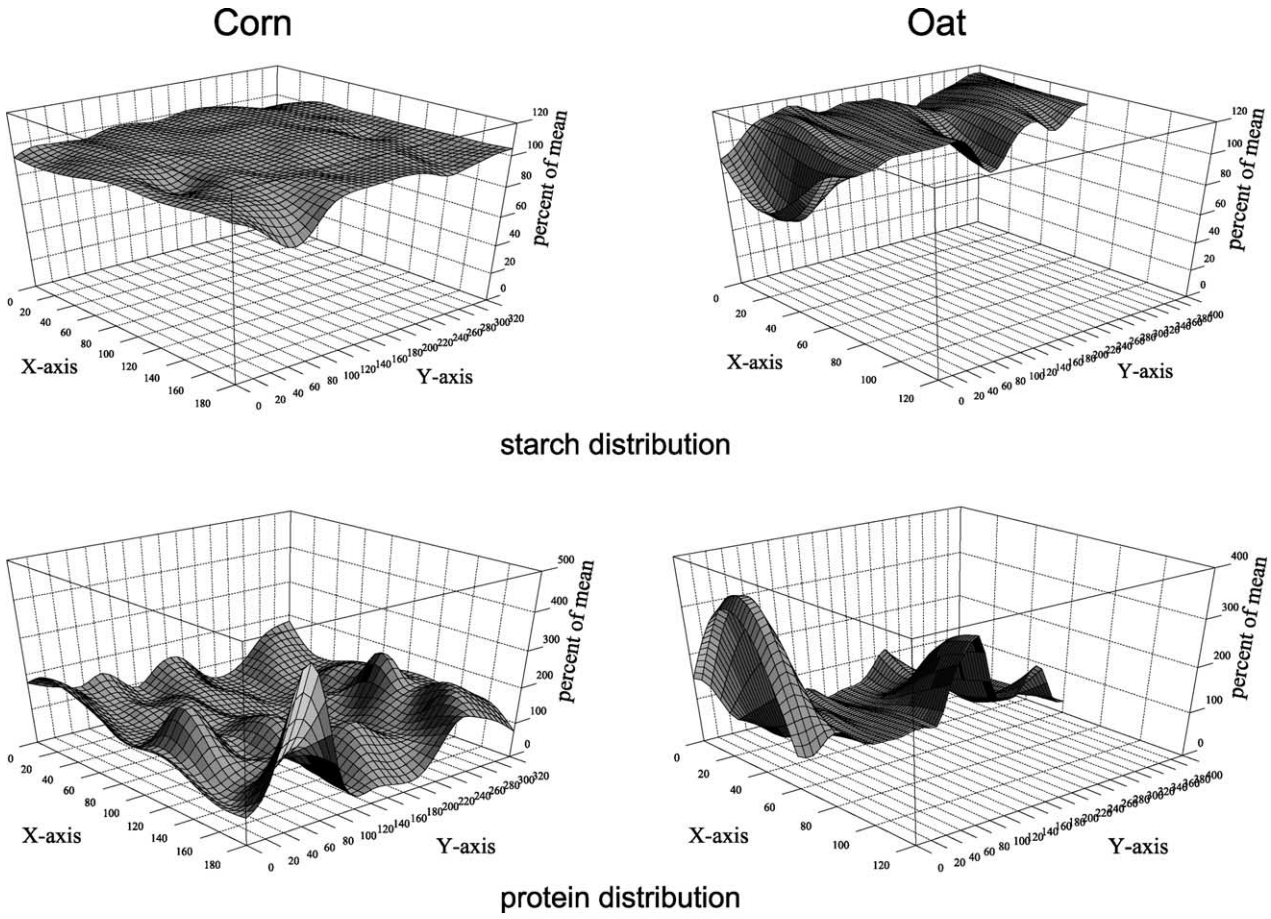

Fig. 5. 3D-surface plot of starch and protein (amide II) distributions in a corn and an oat flour extrudate cross-section (8 μm thickness) showing protein rich spots. Mapping data were acquired at regular intervals of 20 μm. Component concentrations were expressed as percent of the respective mean peak area as averaged from all maps acquired.

heterogeneity of the protein distribution in comparison to the starch distribution. Interestingly, some maps showed distinct spots of a very high protein concentration. At protein-rich spots, the protein concentration reached values that were up to four times higher than the average protein concentration (Fig. 5). The protein rich spots with an estimated diameter of 70 μm are larger than the original protein bodies present in the unprocessed material which were reported to have diameters of approximately 1–20 μm (Batterman-Azcona & Hamaker, 1998; Fulcher, 1986). On the other hand, in the corn and the oat flour extrudates, spectra corresponding to some areas (e.g. corn flour extrudate in Fig. 5 at $x = 180$ μm, $y = 120$–200 μm) did not display a detectable amide II band indicating protein free areas. Fig. 6 shows spectra acquired at three different locations within one map from an oat flour extrudate cross-section. The variability of protein content within a mapped area is apparent from the variation of the amide II band size. The uppermost spectrum showed the most pronounced presence of proteins as can be seen in the amide I and amide II peaks. Moreover this spectrum showed a triangular shaped OH, NH-stretching region (3400–3200 cm^{-1}) which is typical for proteins and is due to the NH-stretching contribution. Note also that the absorbance intensity of the starch region (1100–1000 cm^{-1}) decreased with increasing protein content. Based on data on cereal and soy bean-based extrudates ultrastructure, several investigators proposed that protein bodies rupture during extrusion and aggregate to form a fibrous network in the extrudate (Batterman-Azcona & Hamaker, 1998; Ben-Hdech et al., 1991; Kazemzadeh et al., 1982; Noguchi, 1989). These data point to a more pronounced heterogeneity in the microscopic distribution of protein, which is consistent with the findings of this study except for the reports of aggregated proteins. Our FTIR data did not show a band at frequencies (1615 and 1685 cm^{-1}) corresponding to aggregated state of proteins (Fabian & Schultz, 2000).

3.2.3. Lipid distribution

A fatty acid ester (lipid) distribution was only monitored in the corn/oat and oat flour extrudates since the lipid carbonyl peak was too small for any

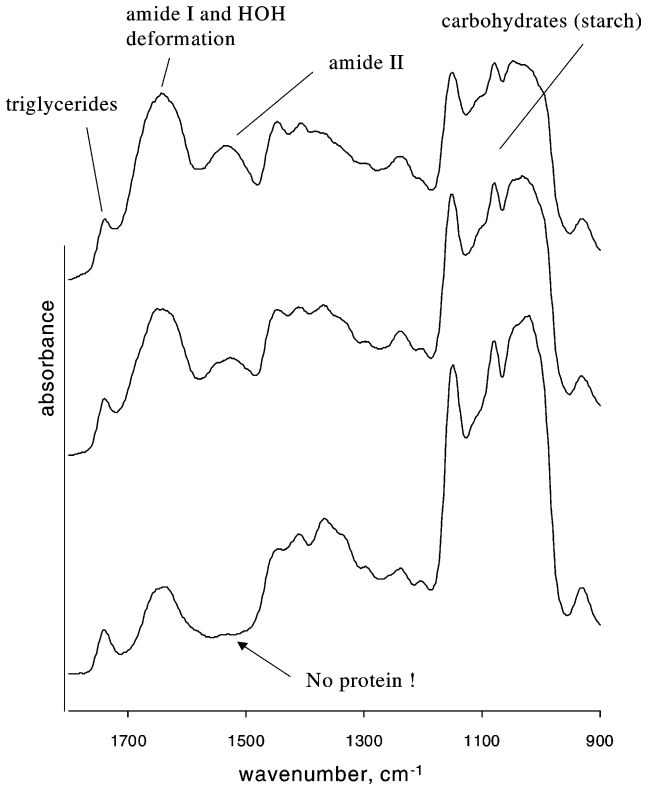

Fig. 6. FTIR spectra of three locations within an oat flour extrudate cross-section (8 μm thickness) differing remarkably in their chemical composition. Spectra were recorded with 20 scans/spectrum and a 67 μm circular aperture.

quantification in the corn flour extrudate (Fig. 1). The degermed corn flour used in this study contained 2.2% lipids. Fig. 7 shows typical lipid distributions encountered in the oat and in the corn/oat flour extrudates. The starch distributions in Fig. 7 are included to allow a comparison with the lipid distribution. The lipid distribution in terms of the RSD was calculated to be16 (corn/oat) and 13% (oat) indicating a less even distribution than the carbohydrates, but more even distribution than the proteins. Within the spatial resolution (around 70 μm) of this study lipid rich domains similar to those protein rich domains could not be observed for the extrudate cross-sections investigated. The absence any detectable lipid rich domains (lipid droplets) may suggest that either such domains may not exist or they may have been smaller than 70 μm.

Ho and Izzo (1992) proposed that lipids could be physically entrapped or encapsulated as droplets or chemically interacting with starch or protein in extrudates. These investigators extracted free and bound lipids from corn meal extrudates before and after α-amylase digestion of the product and further characterized the resulting lipid fractions by HPLC. Free lipids are those that can be extracted from the product by petroleum ether at room temperature whereas bound lipids can be extracted by water-saturated butanol or a chloroform/methanol mixture after having extracted the free lipids. They found out that polar and non-polar lipids are not bound preferentially over the other. They concluded that the lipids are either entrapped or encapsulated by a starch network or entrapped by a starch–protein network as mentioned above. The formation of an amylose–lipid inclusion complex is not expected for the extrudates we studied because the lipids present in the oat flour and the blend of corn and oat flours are mainly triglycerides and do not form amylose–lipid complexes (Lin, Hsieh, & Huff, 1997; Singh & Smith, 1997). Belitz and Grosch (1992) proposed that triglycerides get entrapped by a protein network during bread making. These lipids did not phase-separate when dough was mixed with excess water and ultracentrifuged afterwards. However, they were released and phase-separated when the disulfide bonds in the protein network were reduced to the respective free thiole groups. Guzman, Lee, and Chichester (1992) investigated the binding of the natural lipids of corn during corn meal extrusion and claimed that approximately 2/3 of the free lipids became bound during the given extrusion conditions. The investigators assumed that the interactions leading to lipid binding during extrusion are similar to those observed in the breadmaking process. They also concluded that lipid binding occurred non-selective since they found no difference in the fatty acid distribution in the fraction of the free lipids before and after extrusion.

Several investigators proposed that lipids provide lubrication during extrusion, reduce friction and shear stress and minimize mechanical breakdown of starch granules (Faubion & Hoseney, 1982b; Lin et al., 1997; Singh & Smith, 1997). It is known that extent of shear applied to the material during extrusion can be quantified by SME (Kaletunç & Breslauer, 1996). The decreasing SME values in the order of corn (911 kJ/kg) > corn/oat (547 kJ/kg) > oat (457 kJ/kg) can be attributed to increasing lipid concentration in the raw material. It may be proposed that the lipids distribute in the extruded dough by forming an inner surface film as had been suggested for bread dough (Eliasson & Larsson, 1993).

3.2.4. Comparing component mean values of maps

We conducted statistical analysis for comparison of the mean values of starch, protein, and lipid band areas from three sections (center, peripheral, and middle) of the oat extrudate and the mean values of starch, protein, and lipid band areas from the same section of three extrudates (middle section for corn, corn/oat, oat).

While the mean values of amide II band area varied among three sections (4.4 peripheral, 5.3 center, 6.3 in between), the mean values for carbonyl band (lipid) and carbohydrate band areas were remained the same. Conducting ANOVA and the Kruskal Wallis tests for oat flour extrudate maps showed that p-values are almost zero and are highly significant (<0.0001) for protein

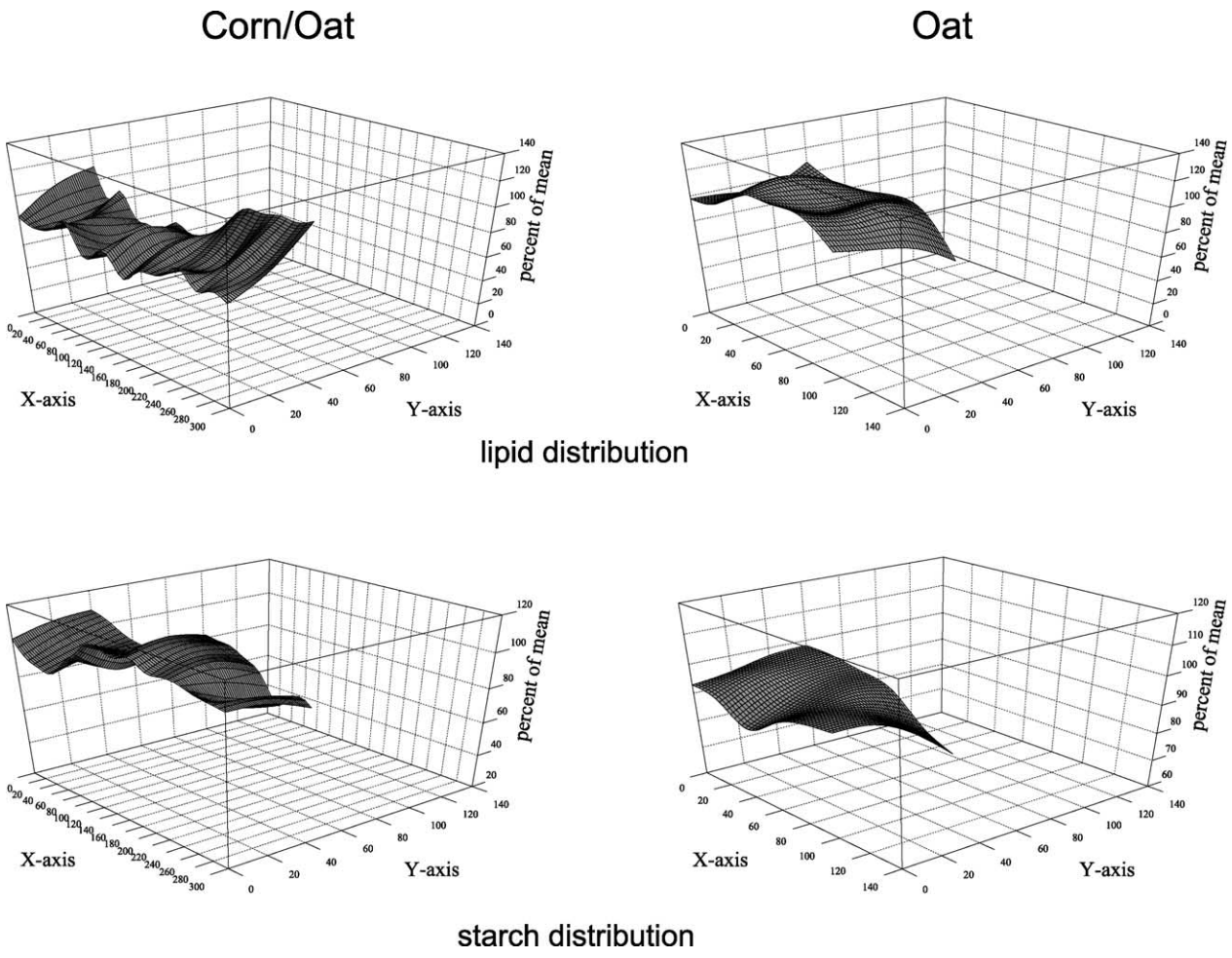

Fig. 7. 3D-surface plot of lipid and starch distribution in two different extrudate cross-sections of 8 μm thickness. Mapping data were acquired at regular intervals of 20 μm. Component concentrations were expressed as percent of the respective mean peak area as averaged from all maps acquired.

indicating significant differences among the mean values of proteins in three sections. For starch and lipid, the Kruskal Wallis test results revealed that the differences were only significant at the 90% confidence level but not at the 95% confidence level. Therefore, statistically the test suggests that differences in the starch and lipid mean values among sections may exist.

ANOVA and Kruskal Wallis tests applied on the mean values of the starch, protein and lipid band areas for the middle section of the different extrudates (corn, corn/oat, oat) revealed that significant differences among extrudate maps existed for proteins and lipids, but not for starch. Comparison of the protein and the starch distributions (Figs. 4 and 5) revealed that in all acquired maps the integrated values of the protein and carbohydrate absorption bands were inversely related. This is also apparent in the spectra shown in Fig. 6. Areas rich in protein had always less starch and vice versa. Statistical analysis of the correlation between carbohydrates and proteins showed existence of a negative correlation between these two components. The correlation coefficients ranged from −0.81 (corn) to −0.91 (oat; mean of the three locations in Fig. 8). Fig. 8A shows the conditioning plot of starch against protein as a function of flour type and location in the extrudate cross-section making the negative correlation apparent.

The lipid distribution seemed to mirror the carbohydrate distribution in some sections of the extrudate microstructure, while in others it did not. The conditioning plot in Fig. 8B shows that slightly positive or negative correlations were observed between starch and lipids. The correlation coefficients ranged from −0.23 to 0.08. Fig. 8C shows the conditioning plot for proteins and lipids which is very similar to the correlation of the starch/lipids (Fig. 8B). The correlation coefficients for protein/lipids ranged from −0.23 to 0.19. The poor correlation coefficients observed for both distribution of starch/lipids and protein/lipids may suggest that the lipid distribution was neither correlated with the carbohydrate nor with the protein distribution. Within the spatial resolution (approx. 70 μm) that was achieved in the present study, the lack of correlation between the distributions of lipids and starch or lipids and proteins may

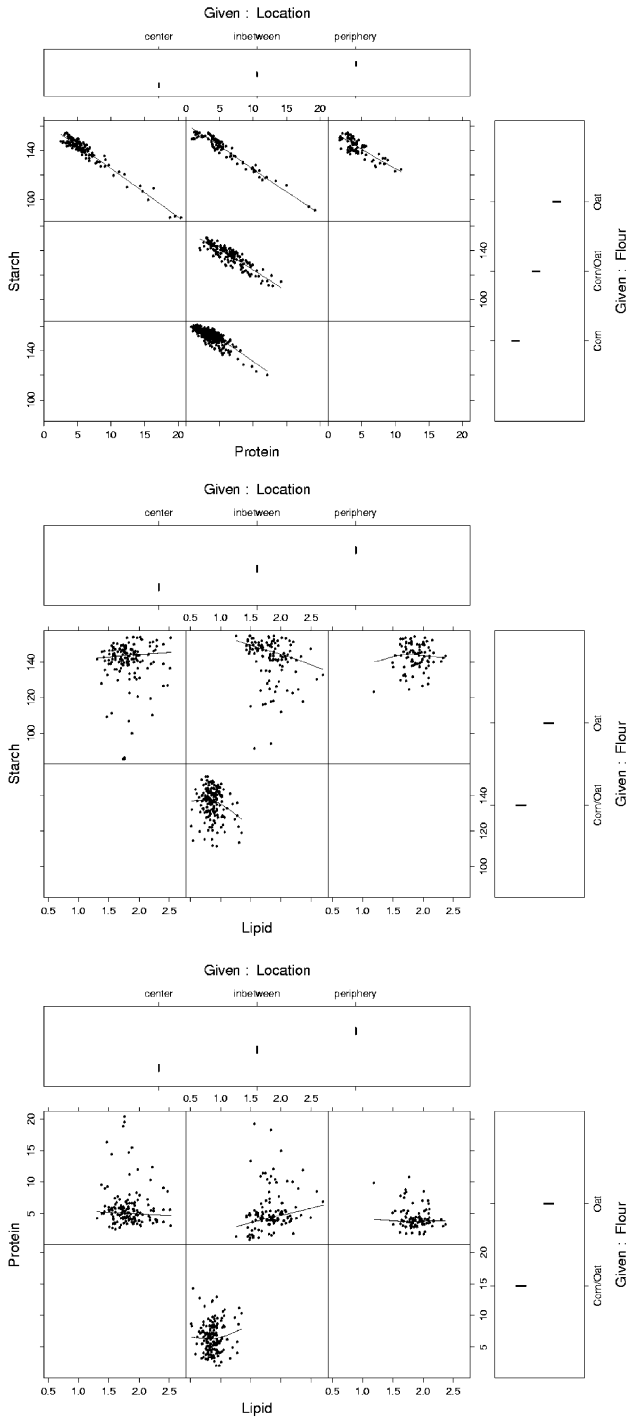

Fig. 8. Conditioning plots of starch against proteins (A), starch against lipids (B) and proteins against lipids (C) in three different extrudate cross-sections made from corn, corn/oat and oat flour. Units at the *x*- and *y*-axis are normalized integration counts of the respective bands from the FTIR spectra. The locations (periphery, middle (inbetween) and center) are different sections within the cross-sections.

suggest an absence of favorable interactions between these pair of components. If favorable interactions occurred, one would expect a positive correlation between lipids and proteins or lipids and starch.

It is important not to overinterpret the correlation patterns we observed, because the correlations depend on the spatial resolution of the mapping experiments. The statistical analysis of the FTIR data indicates a continuous, evenly distributed starch phase formed as a result of extrusion. In contrast, heterogeneity of the protein distribution was observed both among extrudates from various flours and among the various sections (peripheral, middle and center areas) within the same type of extrudate.

4. Conclusions

Structural characterization and the development of structure–physical property relationships are crucial for rational design of process conditions to produce extrudates with desired attributes and storage conditions to enhance stability. Although the importance of structure–property relationships has long been recognized, the information in the literature has been limited to relationships between the macro-cellular structure and the textural properties. This deficiency was due to the lack of appropriate quantitative methods for characterizing microscopic structures in terms of the spatial distribution of biopolymers and moisture.

FTIR microspectroscopy is a non-invasive technique that provides in situ chemical information as a function of position so that an understanding of the structural organization of heterogeneous solid materials at the microstructure level can be developed. Furthermore, quantification of microstructure provides opportunity for the development of useful relationships between the microscopic structures and macroscopic properties such as thermal properties and moisture sorption characteristics.

We have applied the versatile tool of FTIR-microspectroscopy to supplement microscopic structure evaluations of cereal extrudates using light microscopy because FTIR mapping provides quantitative information about the chemical microstructure of the extrudates which is otherwise unavailable. The resultant maps of extrudates allow us to evaluate quantitatively the effects of extrusion processing conditions and formulation on the creation of new microstructures.

FTIR spectra of the corn, corn/oat and oat flour extrudates examined in this study showed similar features. The major observed differences were due to the influence of lipids (CH stretch region, carbonyl band). Spectra of the various extrudates could be distinguished by different peak ratios (amide I/amide II; carbohydrate/amide II) and slight peak shifts for the amide and carbohydrate bands. This investigation of the chemical microstructure of cereal extrudates (made from corn, corn/oat and oat flour) by means of FTIR-microspectroscopy confirmed that carbohydrates (starch) form a continuous phase in the extrudates. Protein was

distributed less uniformly than starch, which is consistent with formation of a protein network during extrusion. Distinct protein rich and protein free domains were observed. The protein rich loci might indicate merging during extrusion processing of protein bodies initially present in flour.

Statistical analysis of the FTIR data confirmed that the uniformity of the distribution of components decreased in the following order starch > lipid > protein. Furthermore, lipid distribution was neither correlated with starch nor with protein distribution implying an absence of favorable interactions between lipid/starch or lipid/protein.

Acknowledgements

We gratefully acknowledge the financial support made available through the University Seed Grant Program (Project number 221934) at the Ohio State University. We also wish to express our appreciation to Dr Christian Schultz from the Bruker Optics Applications Laboratory for his helpful suggestions.

References

Barret, A., Kaletunç, G., Rosenburg, S., & Breslauer, K. (1995). Effect of sucrose on the structure, mechanical strength and thermal properties of corn extrudates. *Carbohydrate Polymers*, *26*, 261–269.

Batterman-Azcona, S. J., & Hamaker, B. R. (1998). Changes occurring in protein body structure and α-zein during cornflake processing. *Cereal Chemistry*, *75*, 217–221.

Belitz, H.-D., & Grosch, W. (1992). *Lehrbuch der lebensmittelchemie*. Berlin: Springer.

Ben-Hdech, H., Gallant, D. J., Bouchet, B., Guegeun, J., & Melcion, J. P. (1991). Extrusion-cooking of pea flour: Structural and immunocytochemical aspects. *Food Structure*, *10*, 203–212.

Bhatnagar, S., & Hanna, M. A. (1994a). Amylose–lipid complex formation during single-screw extrusion of various corn starches. *Cereal Chemistry*, *71*, 582–587.

Bhatnagar, S., & Hanna, M. A. (1994b). Extrusion processing conditions for amylose–lipid complexing. *Cereal Chemistry*, *71*, 587–593.

Chai, W., Disady, L. L., & Rubin, L. J. (1995). Degradation of wheat starch in a twin-screw extruder. *Journal of Food Engineering*, *26*, 289–300.

Chinnaswamy, R., & Hanna, M. A. (1988). Relationship between amylose content and extrusion-expansion properties of corn starches. *Cereal Chemistry*, *65*, 138–143.

Chinnaswamy, R., & Hanna, M. A. (1990). Macromolecular and functional properties of native and extrusion-cooked corn starch. *Cereal Chemistry*, *67*, 490–499.

Chittur, K. K. (1998). FTIR/ATR for protein adsorption to biomaterial surfaces. *Biomaterials*, *19*, 357–369.

Colonna, P., & Mercier, C. (1983). Macromolecular modifications of manioc starch components by extrusion-cooking with and without lipids. *Carbohydrate Polymers*, *3*, 87–108.

Cooper,, & Knutson, (1995). Fourier transform infrared spectroscopy investigations of protein structure. In J. Herron, W. Jiskott, & D. Crommelin (Eds.), *Physical methods to characterize pharmaceutical proteins* (pp. 101–142). New York: Plenum Press.

Durrani, C. M., & Donald, A. M. (1994). Fourier transform infrared microspectroscopy of phase-separated mixed biopolymer gels. *Macromolecules*, *27*, 110–119.

Durrani, C. M., & Donald, A. M. (1995). Compositional mapping of mixed gels using FTIR microspectroscopy. *Carbohydrate Polymers*, *28*, 297–303.

Durrani, C. M., Prystupa, D. A., & Donald, A. M. (1993). Phase diagram of mixtures of polymers in aqueous solution using Fourier transform infrared spectroscopy. *Macromolecules*, *26*, 981–987.

Eliasson, A.-C., & Larsson, K. (1993). *Cereals in breadmaking. A molecular colloidal approach*. New York: Marcel Dekker.

Fabian, H., & Schultz, C. P. (2000). Fourier transform infrared spectroscopy in peptide and protein analysis. In R. A. Meyers (Ed.), *Encyclopedia of analytical chemistry* (pp. 5779–5803). Chichester: Wiley.

Faubion, M., & Hoseney, R. C. (1982a). High-temperature short-time extrusion cooking of wheat starch and flour. I. Effect of moisture and flour type on extrudate properties. *Cereal Chemistry*, *59*, 529–533.

Faubion, M., & Hoseney, R. C. (1982b). High-temperature short-time extrusion cooking of wheat starch and flour. II. Effect of protein and lipid on extrudate properties. *Cereal Chemistry*, *59*, 533–537.

Flint, O. (1994). *Food microscopy: A manual of practical methods, using optical microscopy*. Oxford: BIOS Scientific Publishers Ltd.

Fulcher, R. G. (1986). Morphological and chemical organization of the oat kernel. In F. H. Webster (Ed.), *Oats chemistry and technology* (p. 47) St. Paul, MN: American Association of Cereal Chemists, Inc.

Ghorpade, V. M., Bhatnagar, S., & Hanna, M. A. (1997). Structural characteristics of corn starches extruded with soy protein isolate or wheat gluten. *Plant Foods for Human Nutrition*, *51*, 109–123.

Guzman, L. B., Lee, T.-C., & Chichester, C. O. (1992). Lipid binding during extrusion cooking. In J. L. Kokini, C.-T. Ho, & M. V. Karwe (Eds.), *Food extrusion science and technology* (p. 427) New York: Marcel Dekker.

Hakuli, A., Kytoekivi, A., Lakooma, E.-L., & Krause, O. (1995). FT-IR in the quantitative analysis of gaseous hydrocarbon mixtures. *Analytical Chemistry*, *67*, 1881–1886.

Hermansson, A.-M. (1988). Gel structure of food biopolymers. In J. M. V. Blanshard, & J. R. Mitchell (Eds.), *Food structure—Its creation and evaluation* (p. 25) London: Butterworths.

Ho, C.-T., & Izzo, M. T. (1992). Lipid–protein and lipid–carbohydrate interactions during extrusion. In J. L. Kokini, C.-T. Ho, & M. V. Karwe (Eds.), *Food extrusion science and technology* (p. 415) New York: Marcel Dekker.

Kaletunç, G (1999). FTIR microspectroscopy of wheat extrudate compositional microstructure. *IFT Annual Meeting*, Chicago, IL, July 14–18, 1999, abs. 60–10.

Kaletunç, G., & Breslauer, K. (1996). Construction of a wheat flour state diagram and its application to extrusion processing. *Journal of Thermal Analysis*, *47*(5), 1267–1288.

Kazemzadeh, M., Aguilera, J. M., & Rhee, K. C. (1982). Use of microscopy in the study of vegetable protein texturization. *Food Technology*, *36*(4), 111–118.

Lin, S., Hsieh, F., & Huff, H. E. (1997). Effects of lipids and processing conditions on degree of starch gelatinization of extruded dry pet food. *Food Science and Technology*, *30*, 754–761.

Liu, Y., Hsieh, H., Heymann, H., & Huff, H. E. (2000). Effect of processing conditions on the physical and sensory properties of extruded oat-corn puff. *Journal of Food Science*, *65*(7), 1253–1259.

Maurice, T. J., & Stanley, D. W. (1978). Texture–structure relationships in texturized soy protein IV. Influence of process variables on extrusion texturization. *Canadian Institute of Food Science and Technology Journal*, *11*, 1–6.

Mercier, C., Charbonniere, R., Gallant, D., & Guilbot, A. (1979). Structural modification of various starches by extrusion cooking with a twin-screw French extruder. In J. M. V. Blanshard, & J. R. Mitchell (Eds.), *Polysaccarides in food* (p. 153) London: Butterworths.

Mercier, C., & Feillet, P. (1975). Modification of carbohydrate components by extrusion-cooking of cereal products. *Cereal Chemistry*, *52*, 283–297.

Meuser, F., Pfaller, W., & Van Lengerich, B. (1987). Technological aspects regarding specific changes to the characteristics properties of extrudates by HTST extrusion cooking. In C. O'Connor (Ed.), *Extrusion technology for the food industry* (p. 35) London: Elsevier Applied Science.

Mousia, Z., Farhat, I. A., Pearson, M., Chesters, M. A., & Mitchell, J. R. (2001). FTIR microspectroscopy study of the composition fluctuations in extruded amylopectin–gelatin blends. *Biopolymers (Biospectroscopy)*, *62*, 208–218.

Noguchi, A. (1989). Extrusion cooking of high-moisture protein foods. In C. Mercier, P. Linko, & J. M. Harper (Eds.), *Extrusion cooking* (p. 343) St. Paul, MN: American Association of Cereal Chemists.

Schweizer, T. F., Reimann, S., Solms, J., & Eliasson, A. C. (1986). Influence of drum-drying and twin-screw extrusion cooking on wheat carbohydrates. II. Effect of lipids on physical properties, degradation and complex formation of starch in wheat flour. *Journal of Cereal Science*, *4*, 249–260.

Singh, N., & Smith, A. C. (1997). A comparison of wheat starch, whole wheat meal and oat flour in the extrusion cooking process. *Journal of Food Engineering*, *34*, 15–32.

Skierkowski, K., Gujska, E., & Khan, K. (1990). Instrumental and sensory evaluation of textural properties of extrudates from blends of high starch/high protein fractions of dry beans. *Journal of Food Science*, *55*, 1081–1083. see also page 1087.

Stanley, D. W. (1989). Protein reactions during extrusion processing. In C. Mercier, P. Linko, & J. M. Harper (Eds.), *Extrusion cooking* (p. 321) St. Paul, MN: American Association of Cereal Chemists.

Wetzel, D. L. (1993). Molecular mapping of grain with a dedicated integrated Fourier transform infrared microspectrometer. In G. Charalambous (Ed.), *Food flavors, ingredients and composition* (p. 679) Amsterdam: Elsevier.

Wetzel, D. L., & Fulcher, R. G. (1990). Fourier transform infrared microspectrometry of food ingredients. In G. Charalambous (Ed.), *Flavors and off-flavors* (p. 485) Amsterdam: Elsevier.

Wetzel, D. L., & Reffner, J. A. (1993). Using spatially resolved Fourier transform infrared microbeam spectroscopy to examine the microstructure of wheat kernels. *Cereal Foods World*, *38*(1), 9–20.